Reply to RC1

Newly added figures and their captions:

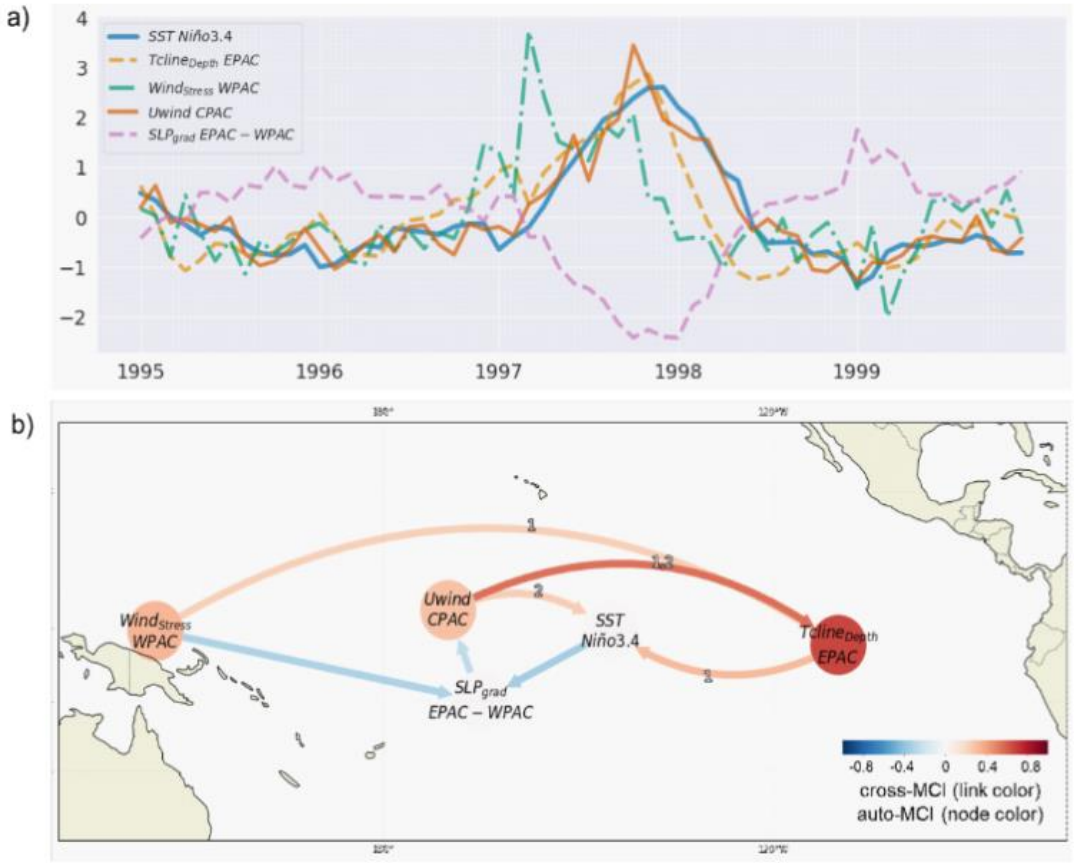

Figure 2. Causal analysis of the for the 1997-1998 El Niño event. a) Detrended standardized monthly time series of the variables listed in Table 1 between 1995-1999. b) Causal network representing lagged (curved) and contemporaneous (straight) causal links, constructed by applying PCMCI+ on the time series in (a). Nodes represent the time series associated with each climate variable (see node labels and details in Table 1). Node colors indicate the self-link strengths of each time series (auto-MCI, see color bar), and the color of the links denotes the cross-link strengths (cross-MCI, see color bar). The link-associated time lags (unit=1 month) are shown as small labels on the links.

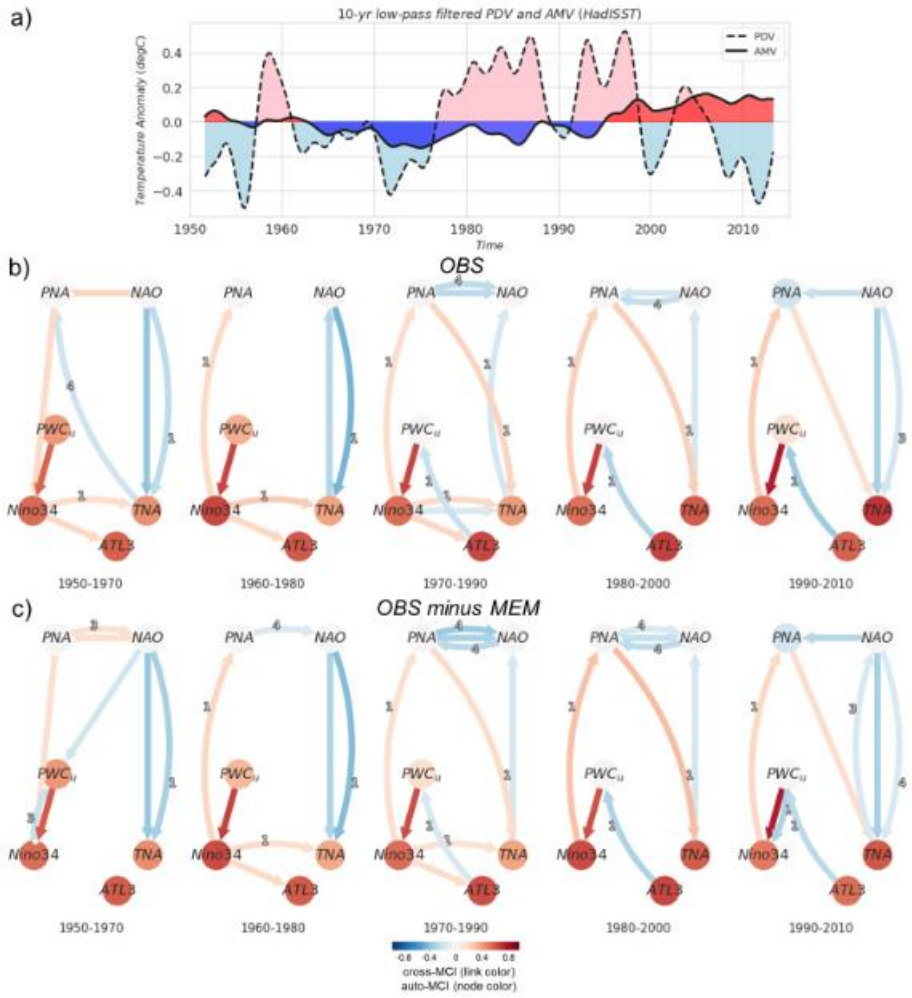

Figure 3. Observed Atlantic-Pacific interactions. a) 10-year low pass-filtered AMV (solid) and PDV (dashed) from the HadISST dataset, calculated following the definition in Sect. 2.4. b) Sliding window analysis where PCMCI+ is applied for five 20-year windows moving by 10 years (see subtitles for each causal graph). In this panel (b, OBS), the algorithm is run on the original time series before removing MEM. The link-associated time lags (unit=1 season i.e 3 months) are shown as small labels on the curved links. c) Similar to (b) but using data where the MEM is removed (OBS minus MEM).

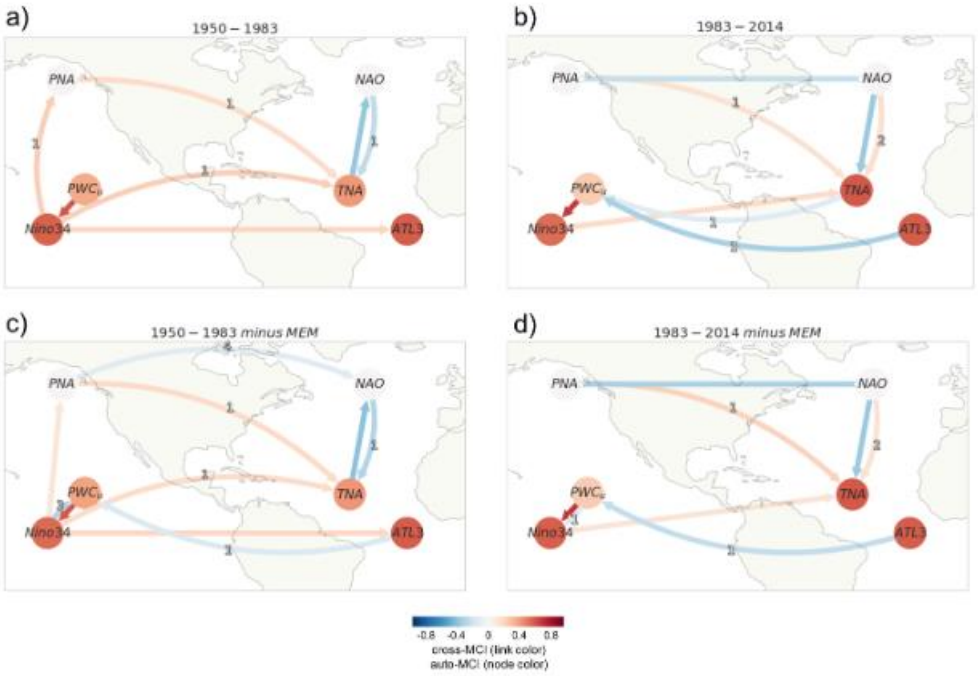

Figure 4. Causal networks representing Atlantic-Pacific teleconnections for 1950-1983 (left column) vs 1983-2014 (right column) in the Reanalyses datasets. (a) Constructed by applying PCMCI+ the 1950-1983 period on the original time series before removing MEM. (b) Same as (a) but for the 1983-2014 period. (c) same as (a), but with indices calculated after removing MEM. (d) Same as (c) but for the 1983-2014 period.

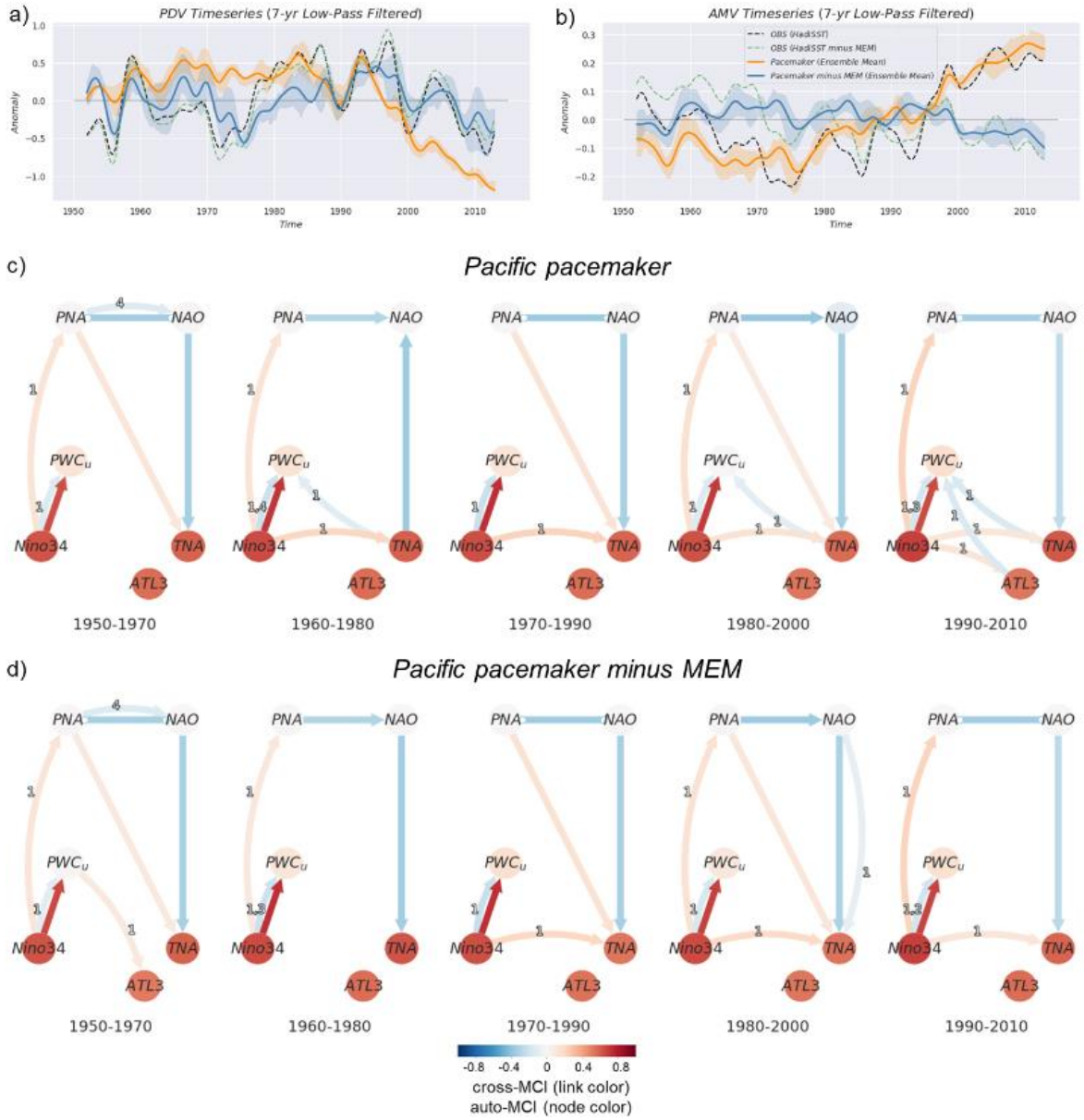
a)
PDV Timeseries (7-yr Low-Pass Filtered)
Anomaly
Time
b)
AMV Timeseries (7-yr Low-Pass Filtered)
OBS (HadISST)
OBS (HadISST minus MEM)
Pacemaker (Ensemble Mean)
Pacemaker minus MEM (Ensemble Mean)
Anomaly
Time
c)
Pacific pacemaker
PNA
NAO
PWC_u
Nino34
TNA
ATL3
1950-1970
1960-1980
1970-1990
1980-2000
1990-2010
d)
Pacific pacemaker minus MEM
PNA
NAO
PWC_u
Nino34
TNA
ATL3
1950-1970
1960-1980
1970-1990
1980-2000
1990-2010
-0.8 -0.4 0 0.4 0.8
cross-MCI (link color)
auto-MCI (node color)

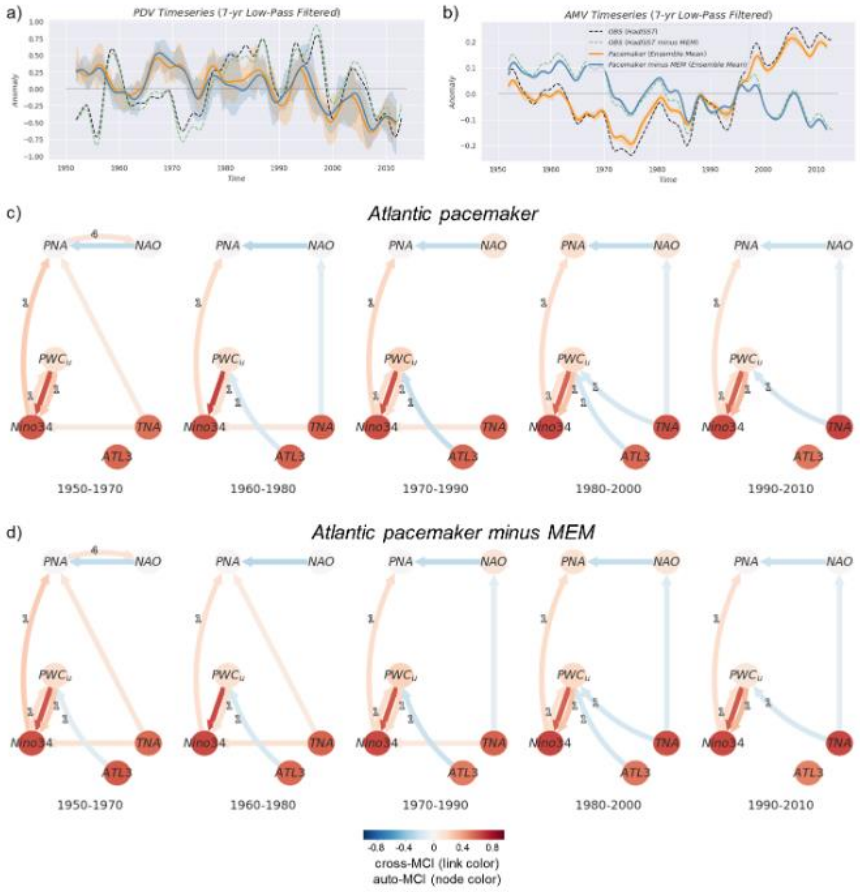

Figure 6. Atlantic pacemaker simulations where North Atlantic SSTAs have been nudged toward observations (see Sect. 2.2). Panels a-d here are similar to Fig. 5a-d but for the Atlantic pacemaker ensemble.

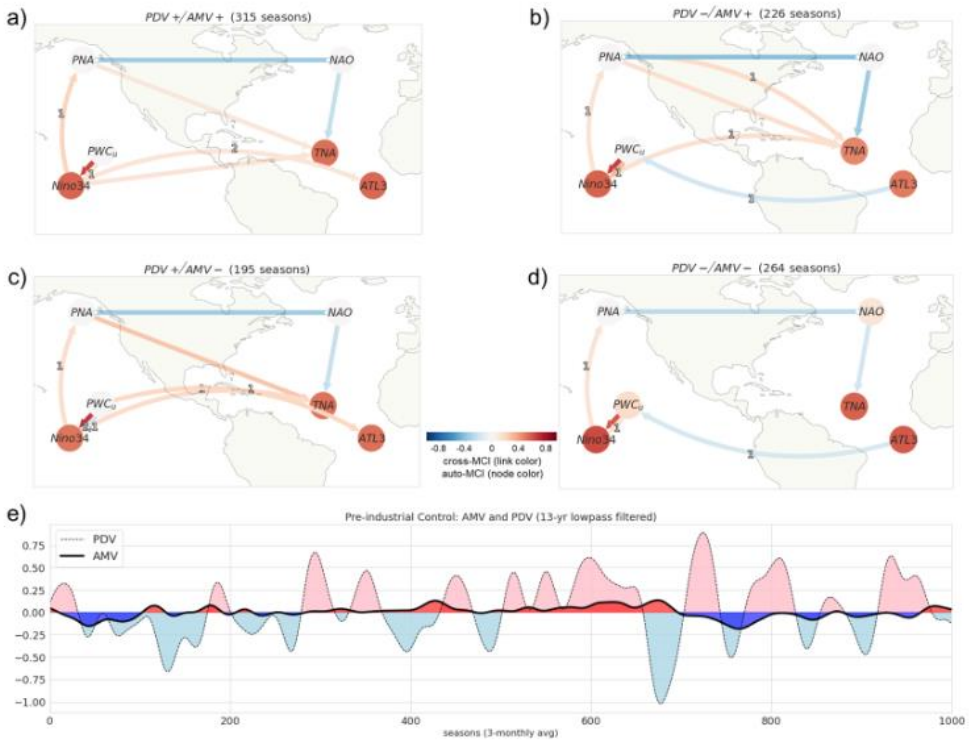

Figure 7. Regime-oriented PCMCI+ analysis of the CESM2 pre-industrial control run. a) Causal graph where only time steps corresponding to either a) PDV+/AMV+, b) PDV-/AMV+, c) PDV+/AMV-, d) PDV-/AMV- regime are considered. The regimes are defined according to the phase of e) smoothed AMV and PDV indices (13-year low-pass filtered) illustrating the decadal internal variability over the Atlantic and Pacific for 250 years (1000 time steps [seasons (3-monthly averages)]. Positive (negative) phases are shaded in pink (light blue) and red (blue) for PDV and AMV, respectively.)

Changing effects of external forcing on Atlantic-Pacific interactions

Soufiane Karmouche[1,2], Evgenia Galytska[1,2], Gerald A. Meehl[3], Jakob Runge[4,5], Katja Weigel[1,2], and Veronika Eyring[2,1]

[1]University of Bremen, Institute of Environmental Physics (IUP), Bremen, Germany
[2]Deutsches Zentrum für Luft- und Raumfahrt e.V. (DLR), Institut für Physik der Atmosphäre, Oberpfaffenhofen, Germany
[3]Climate and Global Dynamics Laboratory, National Center for Atmospheric Research (NCAR), Boulder, CO, USA
[4]Deutsches Zentrum für Luft- und Raumfahrt e.V. (DLR), Institut für Datenwissenschaften, Jena, Germany
[5]Fachgebiet Klimainformatik, Technische Universität Berlin, Berlin, Germany

Correspondence: Soufiane Karmouche (sou_kar@uni-bremen.de)

List of Figures

1 Supplementary Material for Section 3.2.1 (Proof of Concept)

Figures S1 and S2 show two of the pre-processing steps taken to decide the conditional independence test (Fig. S1) and the maximum time lag τ_{max} (Fig. S2) during the PCMCI+ analysis. The non-Gaussian marginal distribution of the time series and the use of *RobustParcorr* is only applicable for Sect. 3.2.1. The density plots for the data used in Sect. 4 (not shown) did not reveal such distributions, hence, *Parcorr* was used as conditional independence test there. Similar to Fig. S2, the lag function plots for the variables in Sect. 4 (not shown) are analyzed to decide τ_{max}. Except for a PNA-NAO connection at 8-season lag (having no physical basis), all dependencies decay after a maximum lag of 4 time lag steps, hence the use of $\tau_{max} = 4$ seasons.

Figure S3 shows the p-values (uncertainty) associated with the PCMCI+ estimated coefficients during the proof-of-concept analysis shown in Fig. 2.

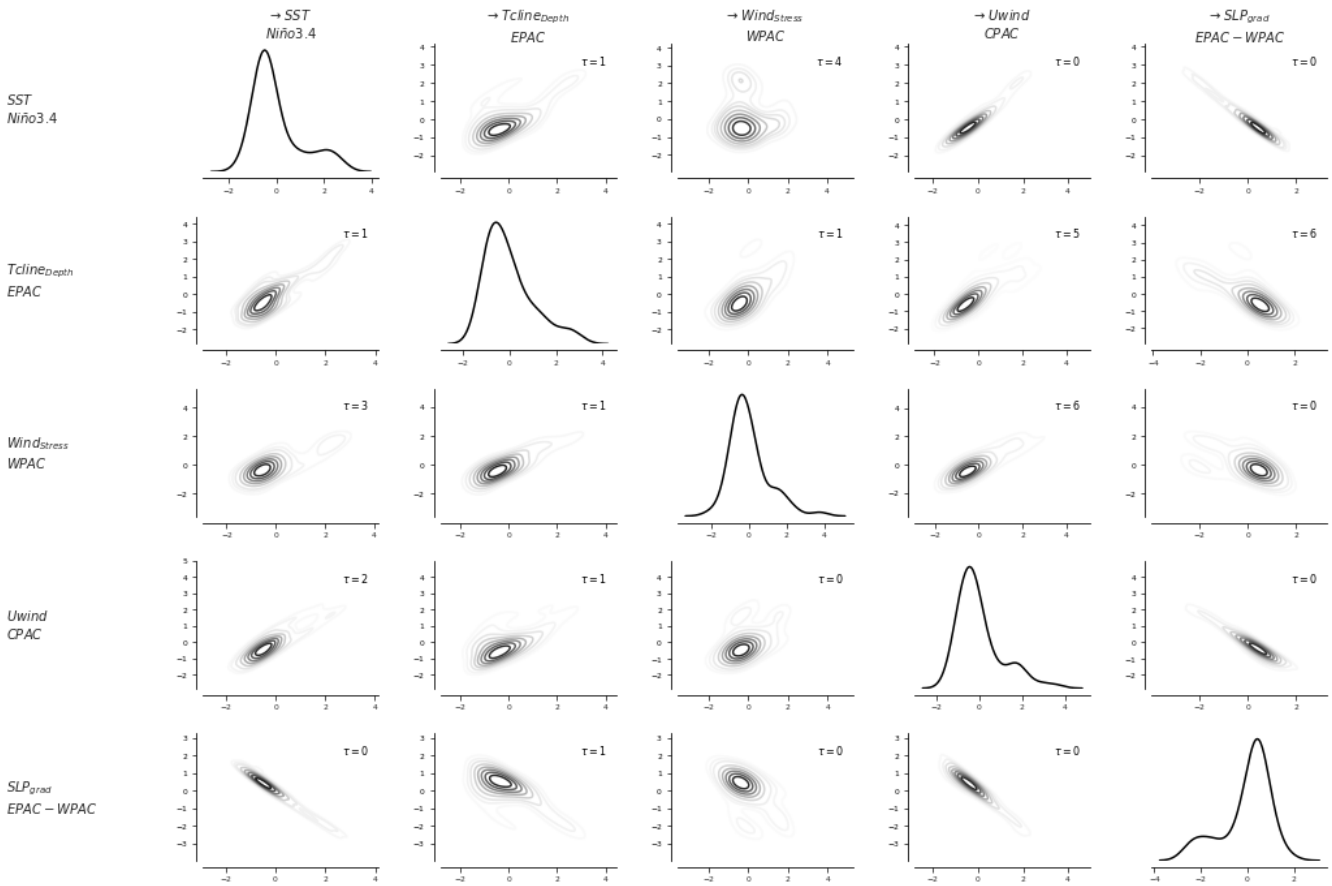

Figure S1. Density plots derived from kernel density estimation (analogous to histograms) are shown off-diagonal. Along the diagonal, the marginal distributions are non-Gaussian for most variables. As mentioned in Sect 3.2, the skewed distributions are handled with the *RobustParcorr* conditional independence test in the proof of concept (Sect. 3.2.1).

2 Supplementary Material for Section 4

In this supplementary section, we show the averaged time series of the six variables used in the analysis of Atlantic-Pacific interactions (Sect. 4.2) for the Pacific pacemaker ensemble (Fig. S4) and the Atlantic pacemaker ensemble (Fig. S5). The p-value matrices for the PCMCI+ estimated dependencies (the coefficients in all causal graphs) in Sect. 4. These present an uncertainty measure of the respective cross(auto)-MCI coefficients. The links shown on the causal graph have p-values lower than α_{pc} and are shown in red in the odd-numbered Figs S7-15. The significant threshold α_{pc} is set to 0.2 in Sect. 4.1, 0.01 in Sect. 4.2,

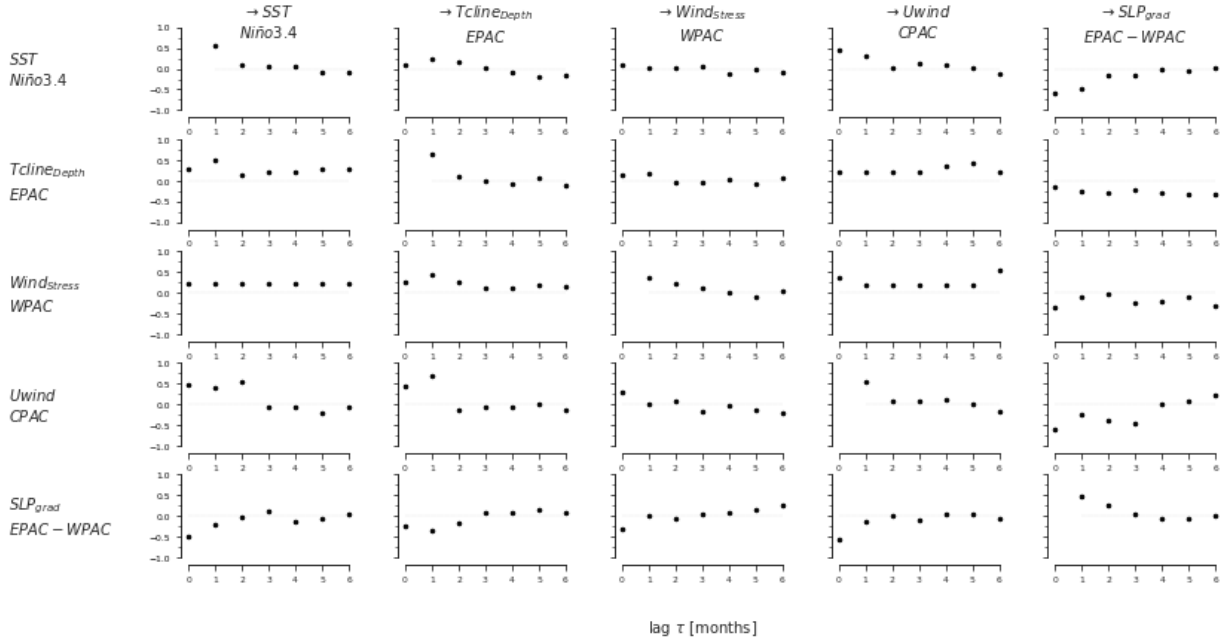

Figure S2. Lag function plot showing the lagged dependencies between the variables in Sect. 3.2.1 for six months. Most dependencies decay by $\tau = 3$ time steps, hence the choice for $\tau_{max} = 3$ [months] in the proof of concept (Sect. 3.2.1).

and 0.05 in Sect. 4.3. We also show in the even-numbered Figs S6-14, the causal graphs obtained through PCMCI+ when no background knowledge is introduced. As discussed in methods (Sect. 3), the PCMCI+ networks might contain conflicting links ($X_i^t \times - \times X_j^t$) at lag zero. The potential differences between the links shown here (Supplementary material) and the ones on the main manuscript lie in the adjacencies that were not considered by PCMCI+ due to the assumptions introduced and listed in Sect. 3.2.2 (based on background knowledge, sensitive analyses, and inspection of the conflicting edges).

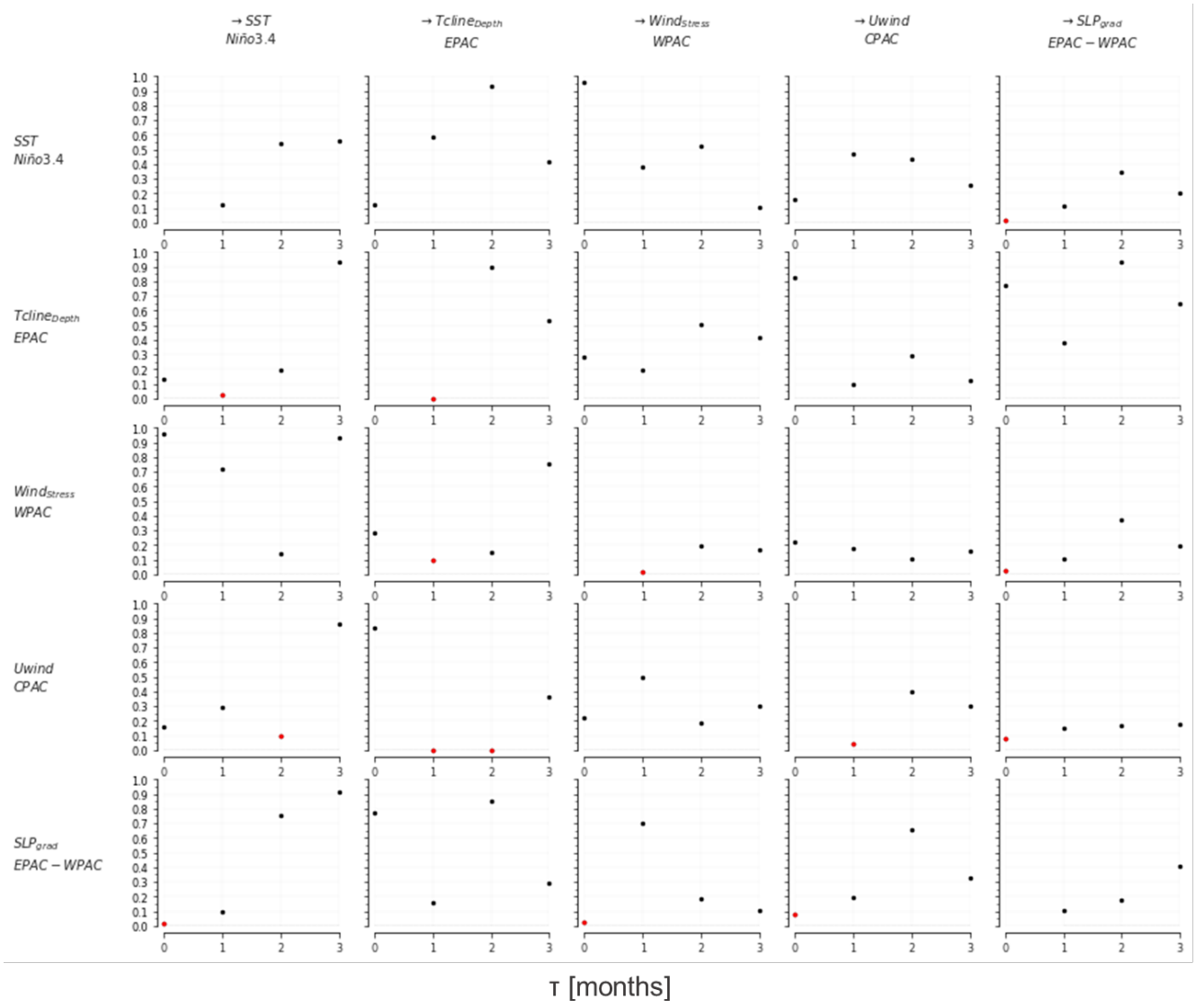

Figure S3. Lagged p-value matrix for the cross-MCI coefficients in the causal graph shown Fig. 2b. The x-axis of each scatter subplot shows the time lag from $\tau_{min} = 0$ to $\tau_{max} = 3$ [months]. The p-values are shown on the y-axis for each pair (see variable names left and top of each subplot) and denote the uncertainty of each estimated dependency. The p-values below the significance threshold α_{pc} (here α_{pc}=0.1) are shown in red.

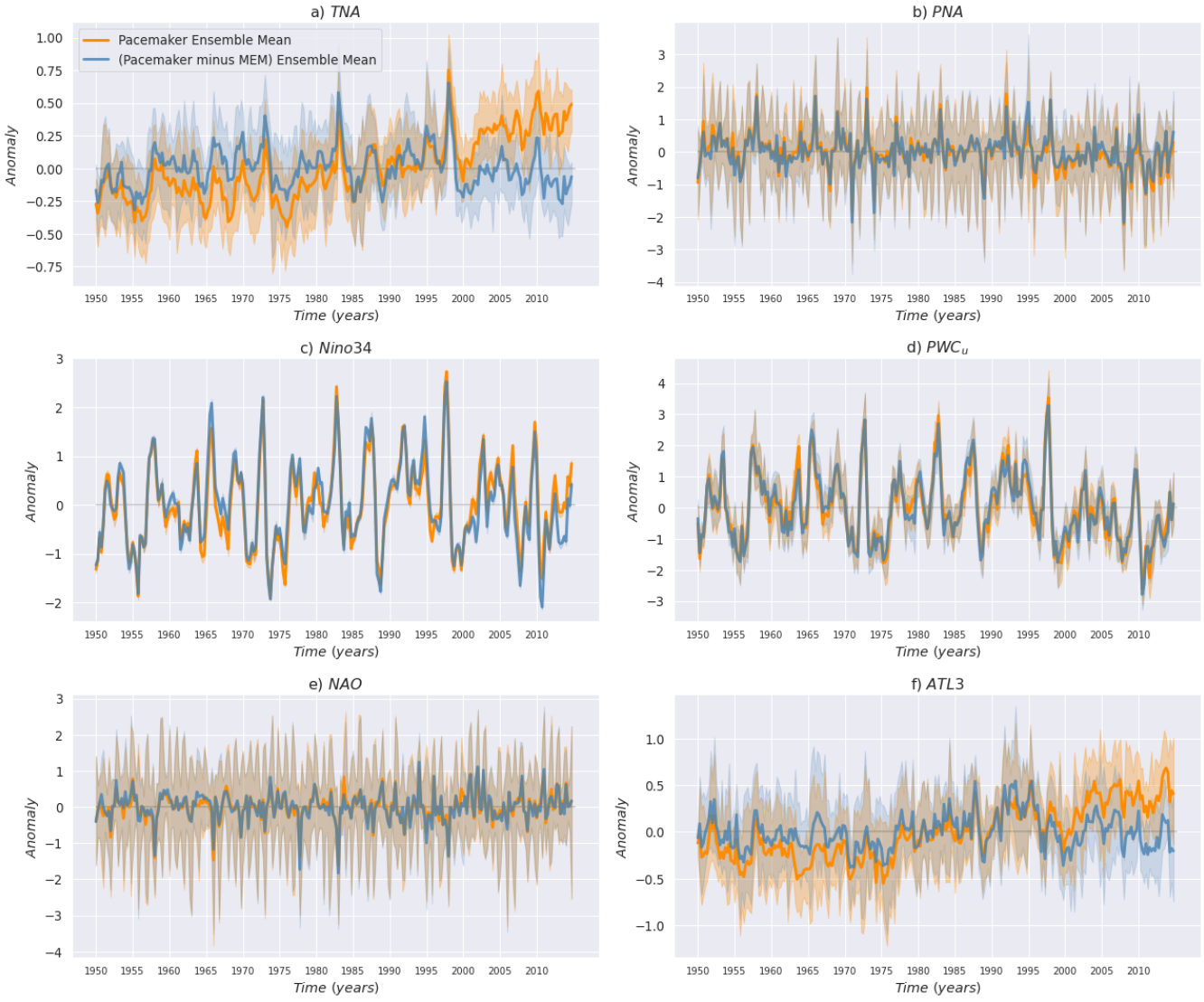

Figure S4. Ensemble-averaged indices from the Pacific pacemaker ensemble (10 members) for a) TNA, b) PNA, c) Niño3.4, d) PWCu, e) NAO, and f) ATL3 for the 1950-2014 period. The time series in orange (blue) represent the indices calculated before (after) subtracting MEM. Shadings denote the 25th-75th percentile range.

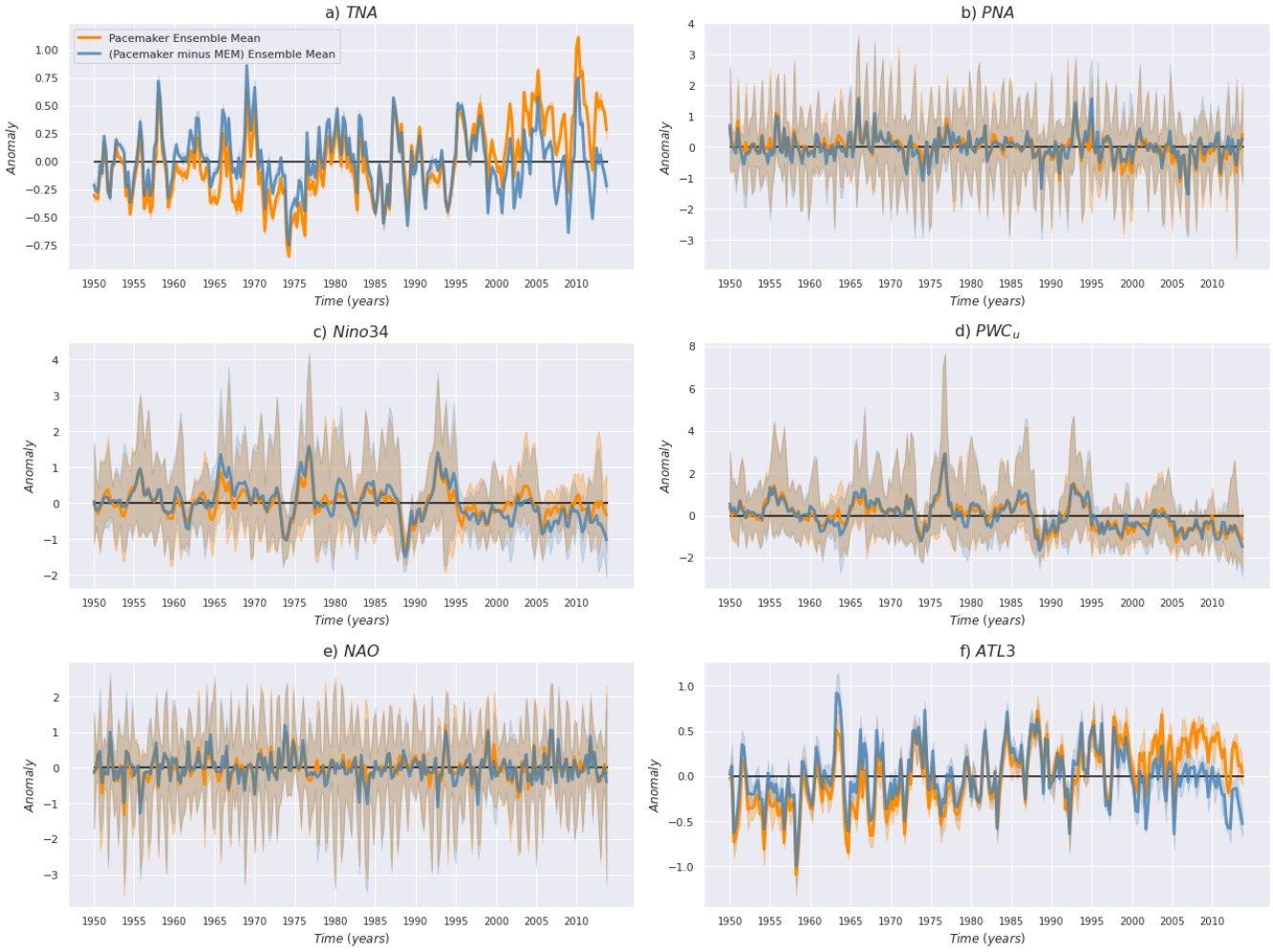

Figure S5. Same as Fig. S4 but for the Atlantic pacemaker ensemble (10 members) for the 1950-2013 period.

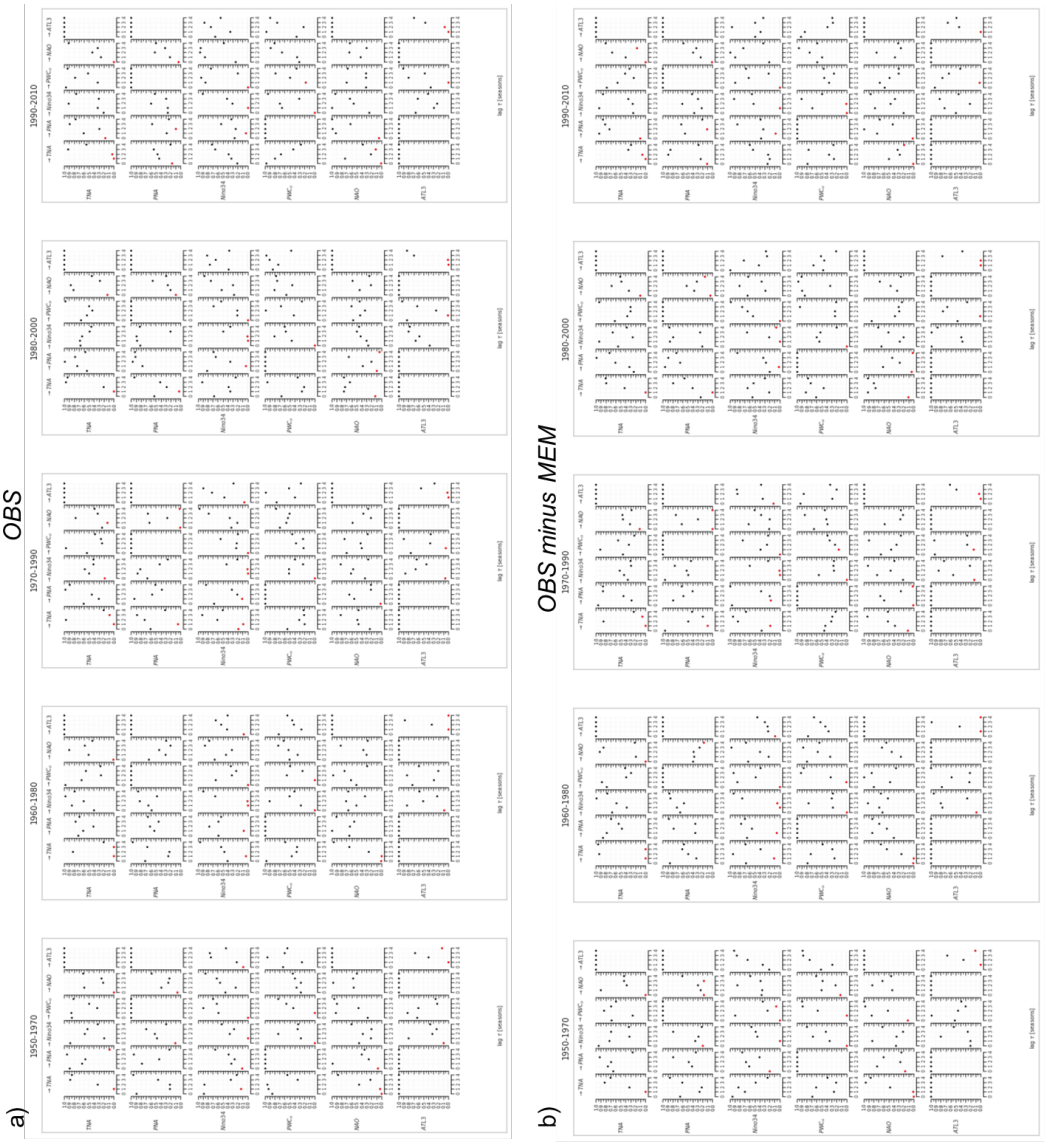

Figure S6. Lagged p-value matrices for the coefficients on the causal graphs shown in Fig. 3b and c. The Figure is rotated 90° to the left to fit the page format. a) The are five subplots for the five windows analyzed in each panel (see corresponding Fig 3b) each resembling the p-values matrix shown in Fig. S3 but for the indices and parameters used in Sect. 4.1. Here, $\tau_{min} = 0$ and $\tau_{max} = 4$ [seasons i.e. 3-monthly averages]. The p-values below the significance threshold α_{pc} (here α_{pc}=0.2) are shown in red. Panel (a) corresponds to causal graphs in Fig. 3b (OBS, see the title and corresponding subtitles in Fig. 3b for each window period). The pairs of adjacencies that were not estimated following assumptions (listed in Sect. 3.2.2) have p-values approaching 1. b) Same as (a) but correspond to graphs shown in Fig. 3c (OBS minus MEM).

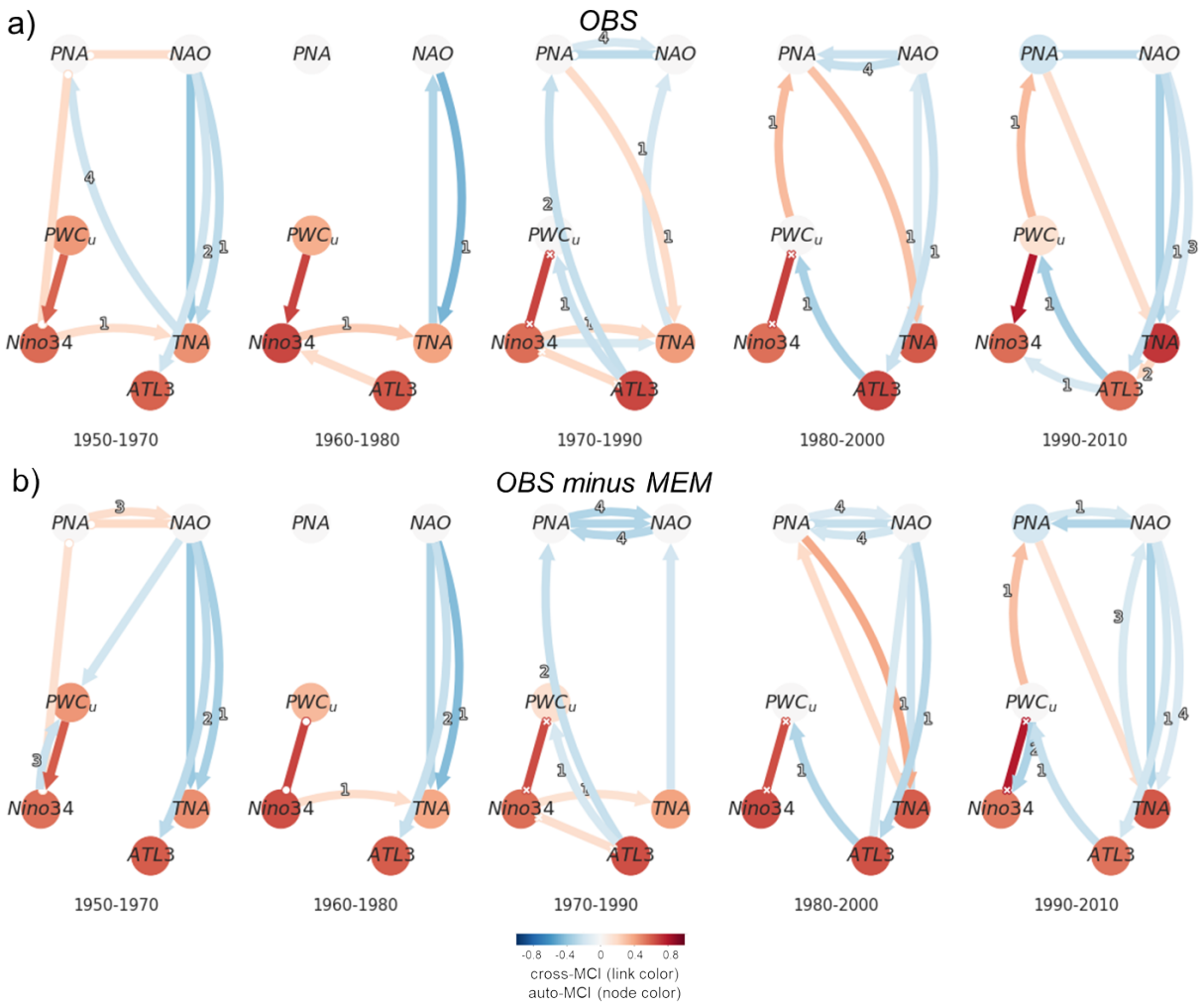

Figure S7. Causal graphs with no background knowledge. a) PCMCI+ causal networks corresponding to the ones shown in Fig. 3b obtained when no assumptions are introduced i.e. all dependencies between all variables at all lags (up to τ_{max}) are considered. These might contain conflicting ($X_i^t \times - \times X_j^t$). b) Same as (a) but for the causal graphs of Fig. 3c.

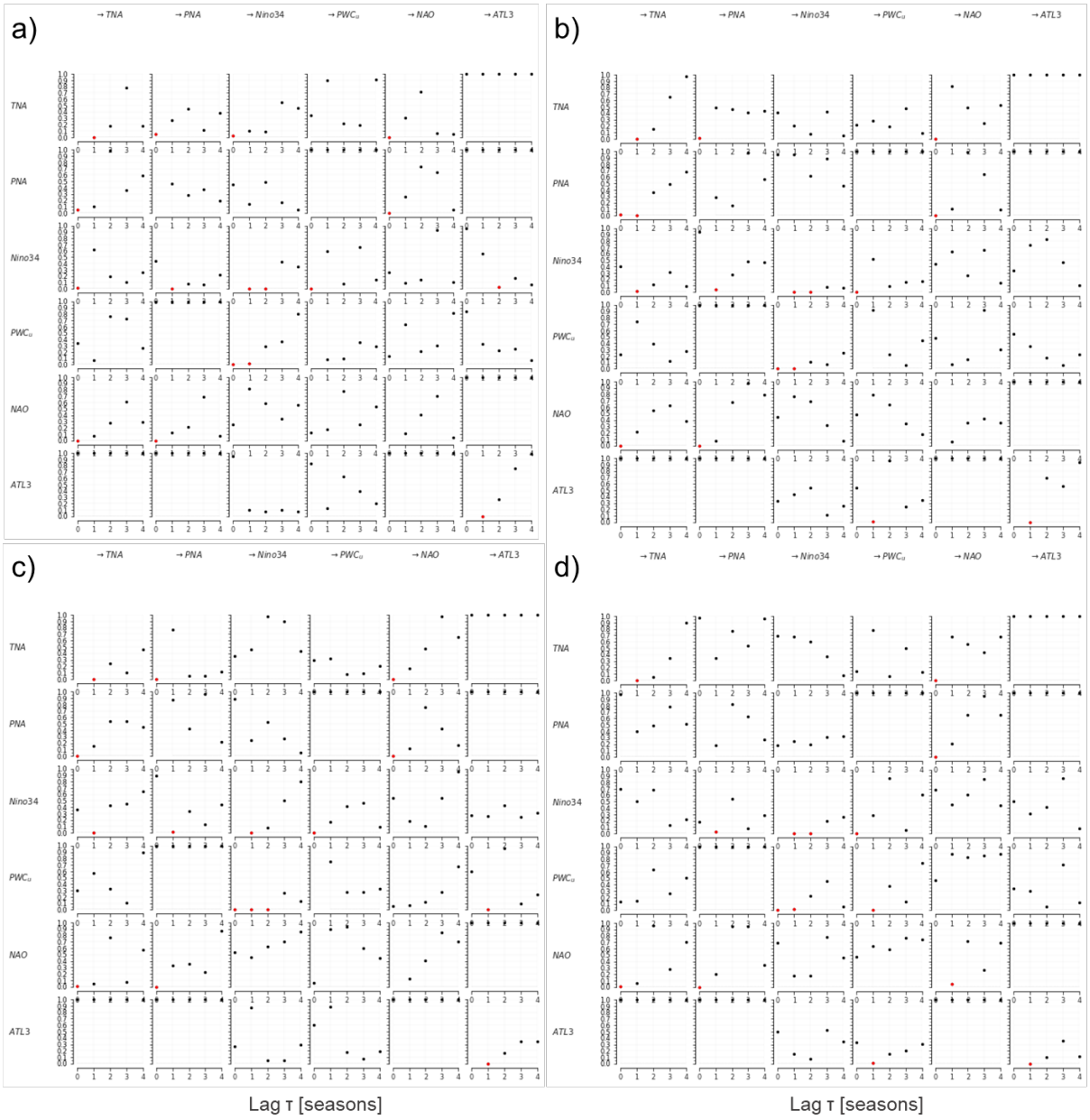

Figure S8. Similar to Figs S3 and S6 but for causal graphs shown Fig 4 (panels a-d here correspond to panels a-d in Fig. 4). Significance threshold α_{pc} is set to 0.2 here.

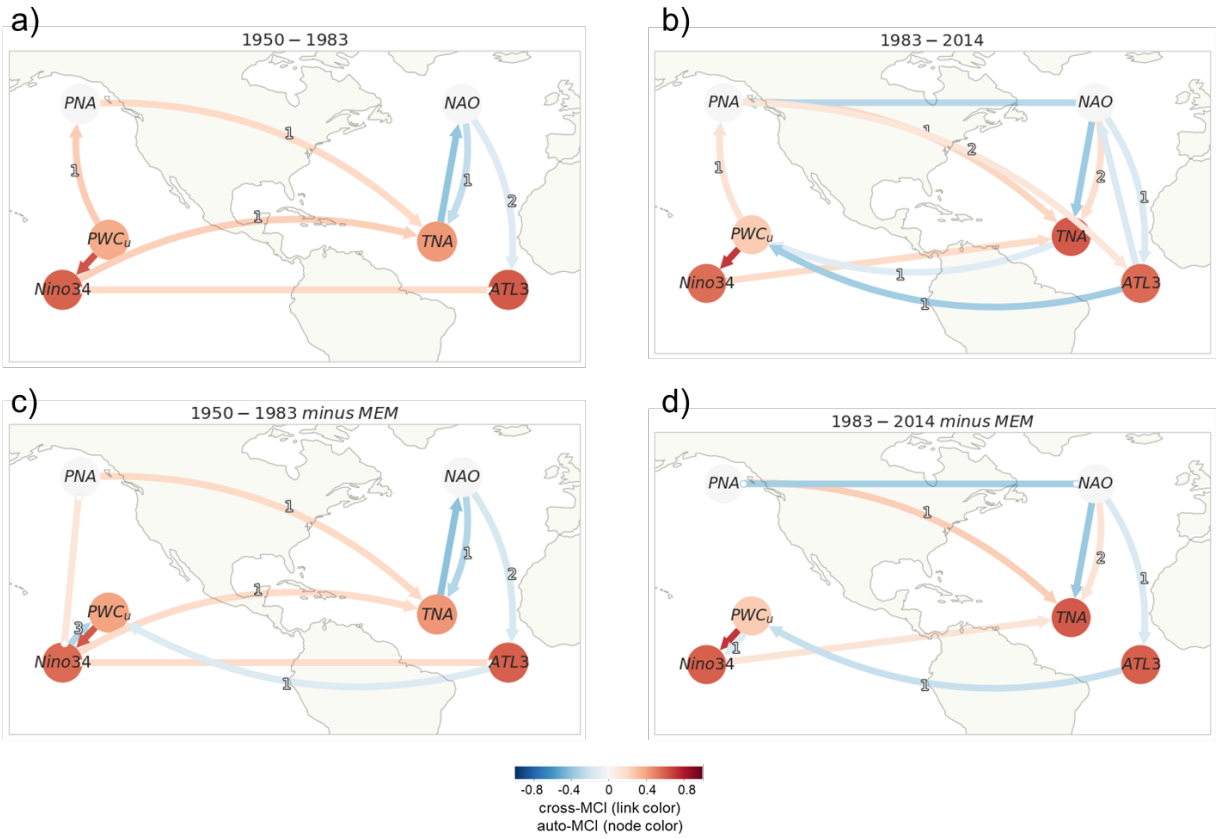

Figure S9. Similar to Fig. S7 but for the causal graphs in Fig. 4 (panels a-d here correspond to panels a-d in Fig. 4).

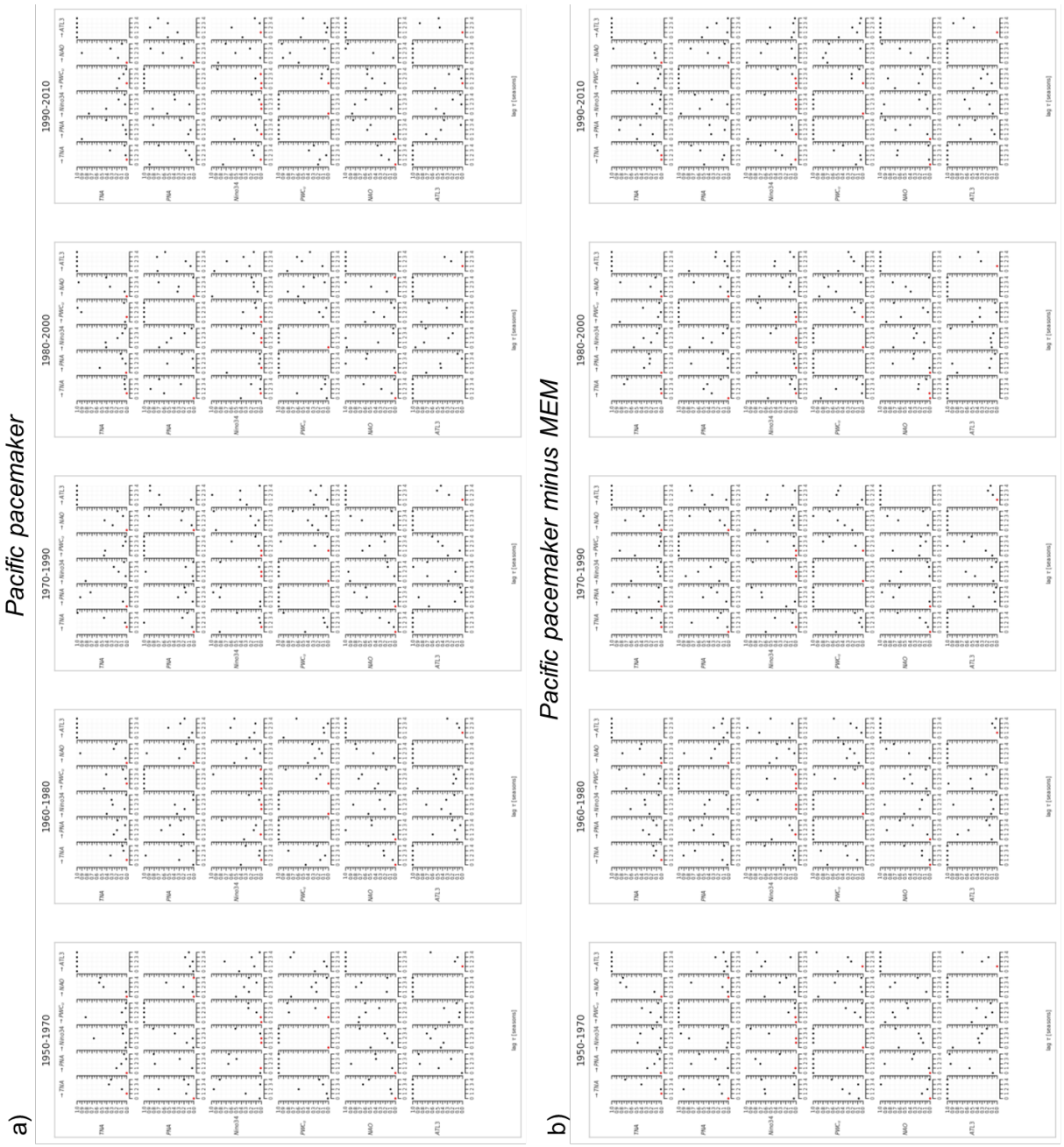

Figure S10. Similar to Figs S6 but for causal graphs shown Fig. 5b and c. The significance threshold α_{pc} is set to 0.01 here.

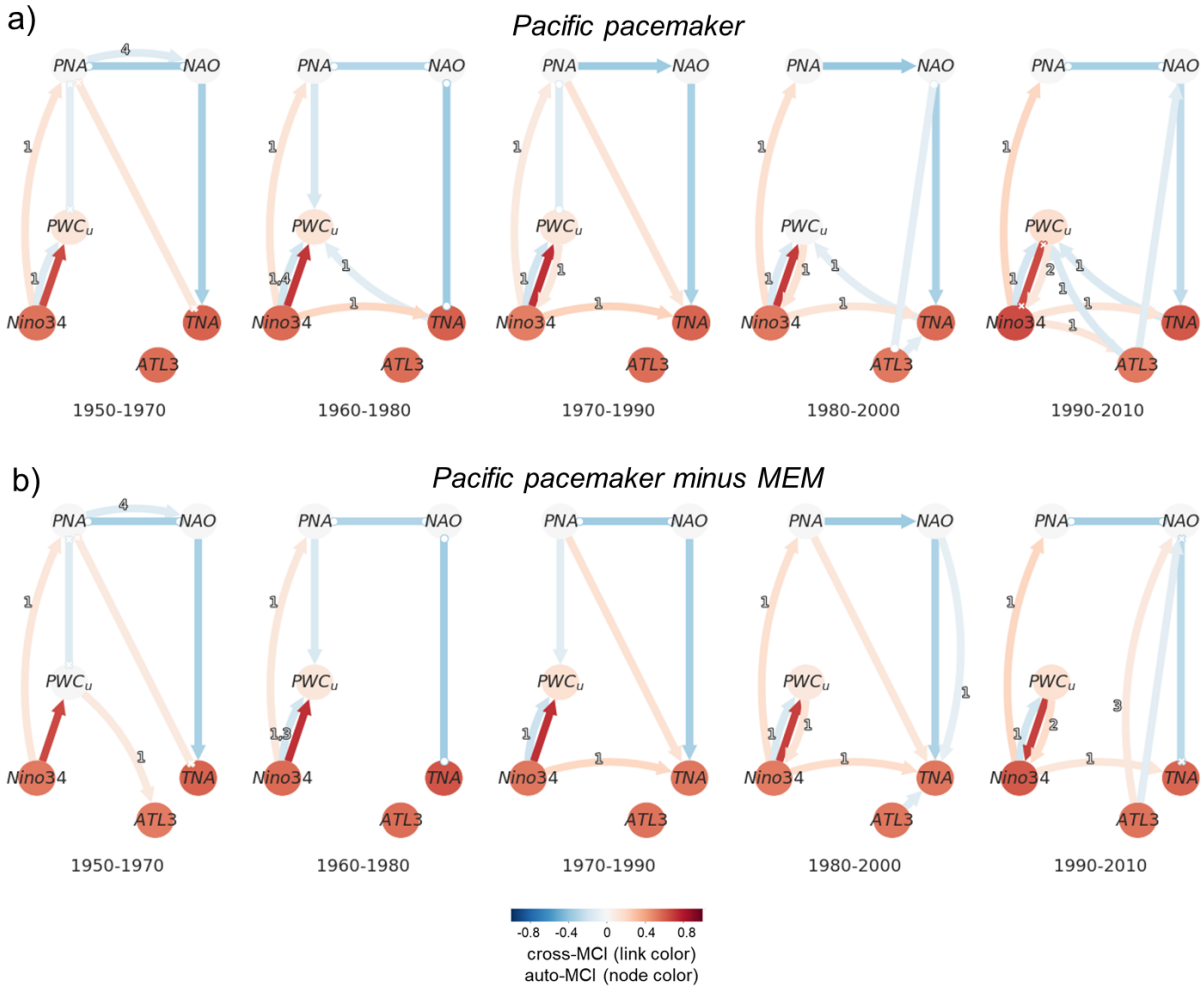

Figure S11. Similar to Fig. S7 but for the causal graphs in Fig. 5b and c.

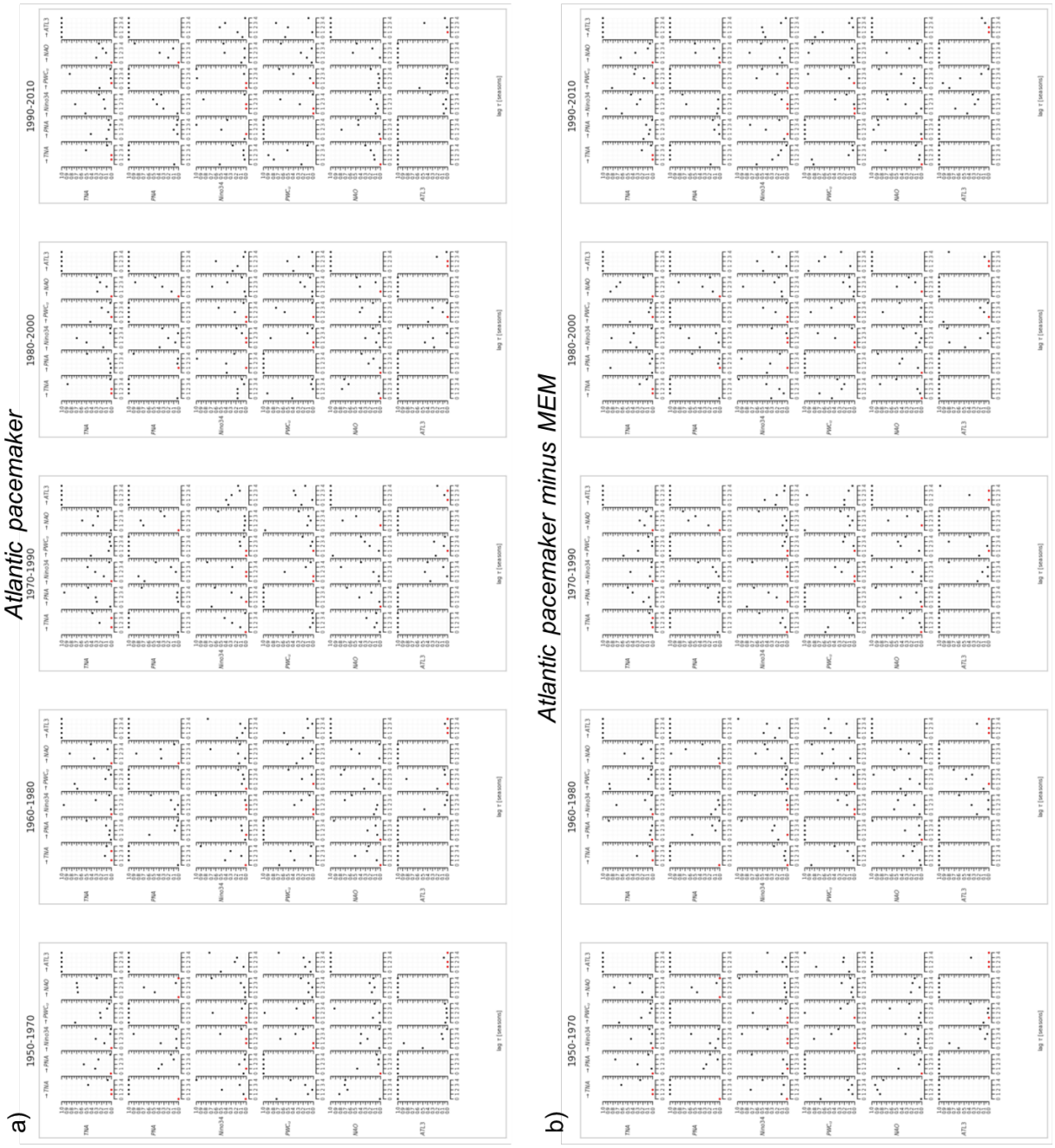

Figure S12. Similar to Figs S6 but for causal graphs shown Fig. 6b and c. The significance threshold α_{pc} is set to 0.01 here.

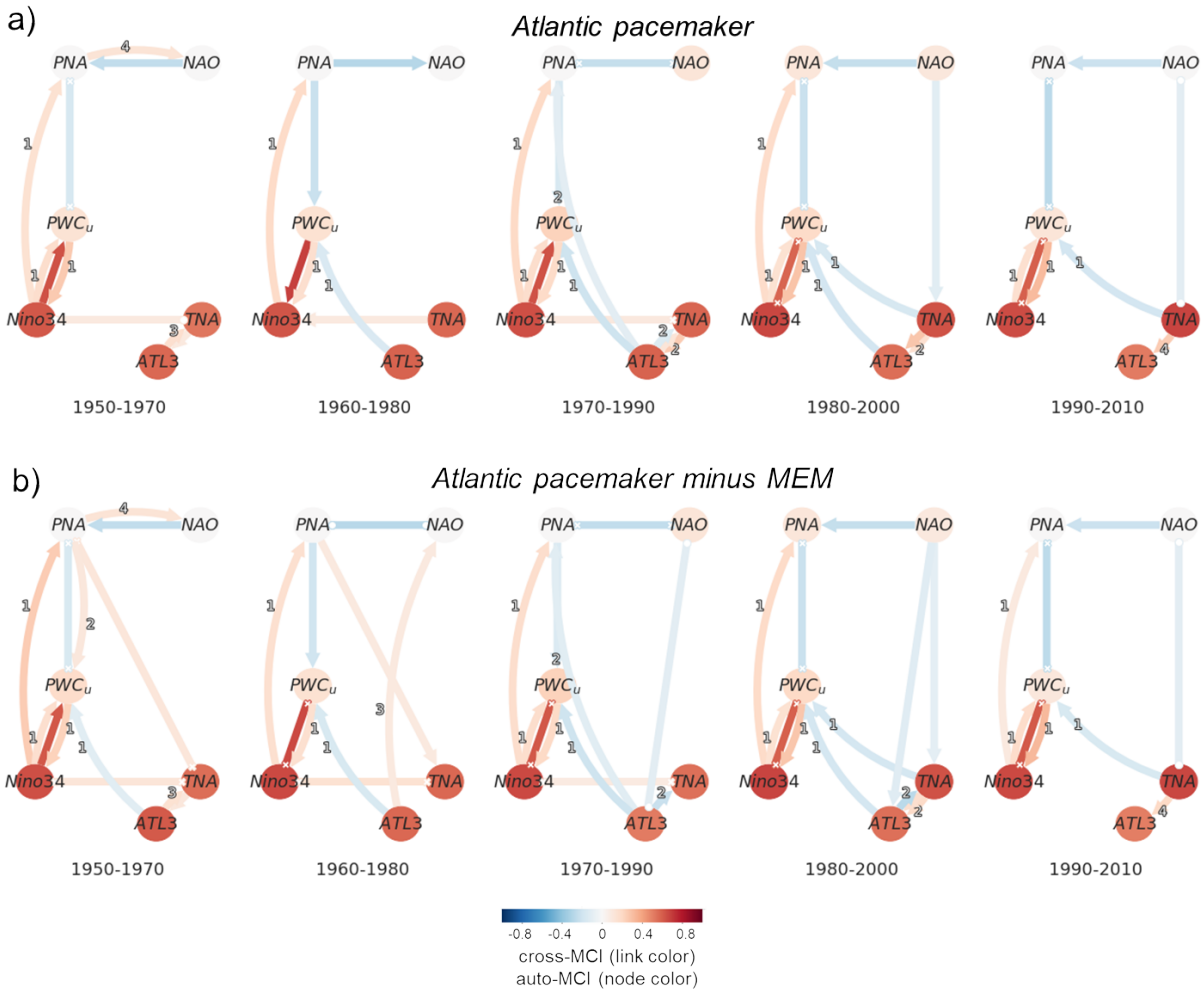

Figure S13. Similar to Fig. S7 but for the causal graphs in Fig. 6b and c.

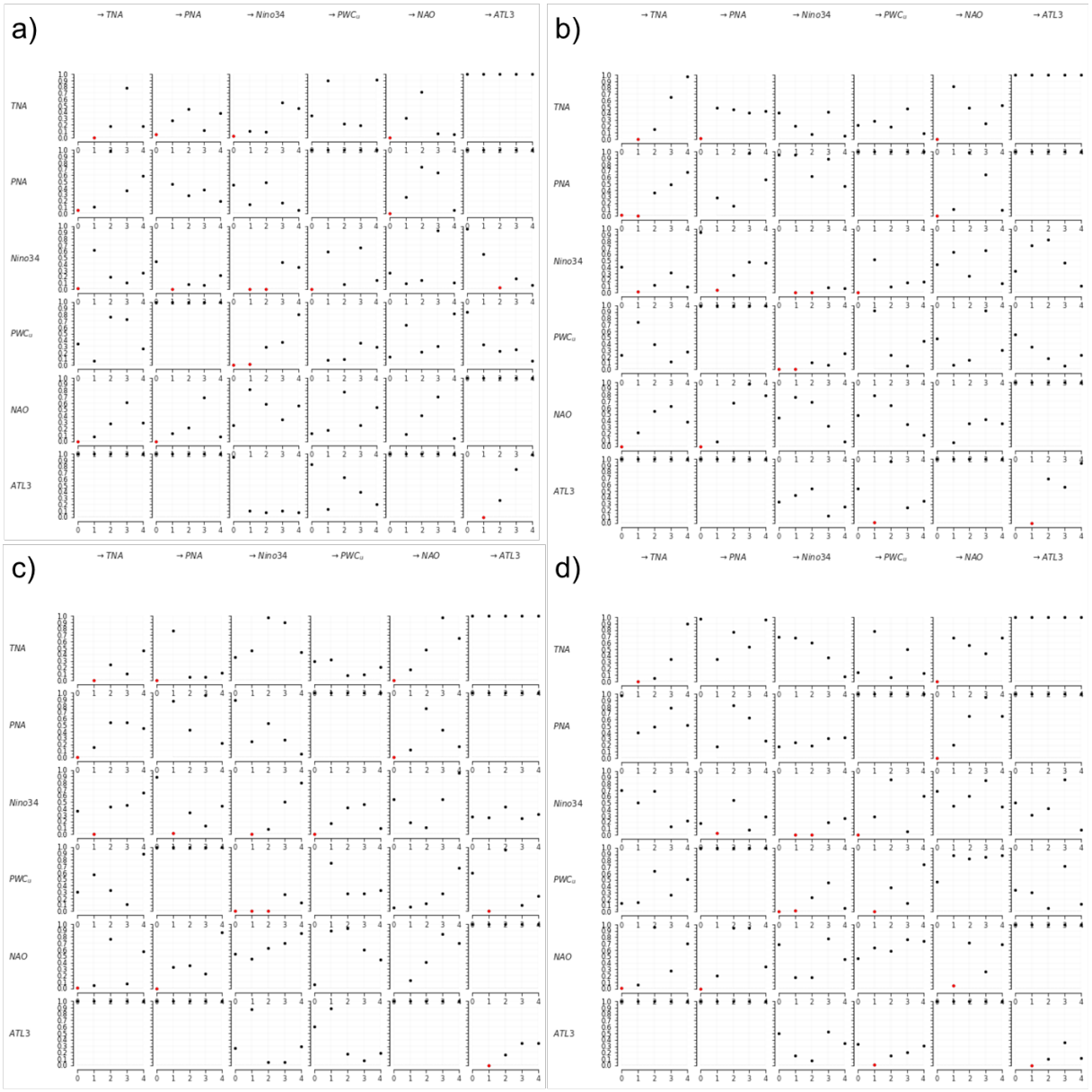

Figure S14. Similar to Fig. S6 but for the causal graphs shown in Fig. 7a-d. The significance threshold α_{pc} is set to 0.05 here.

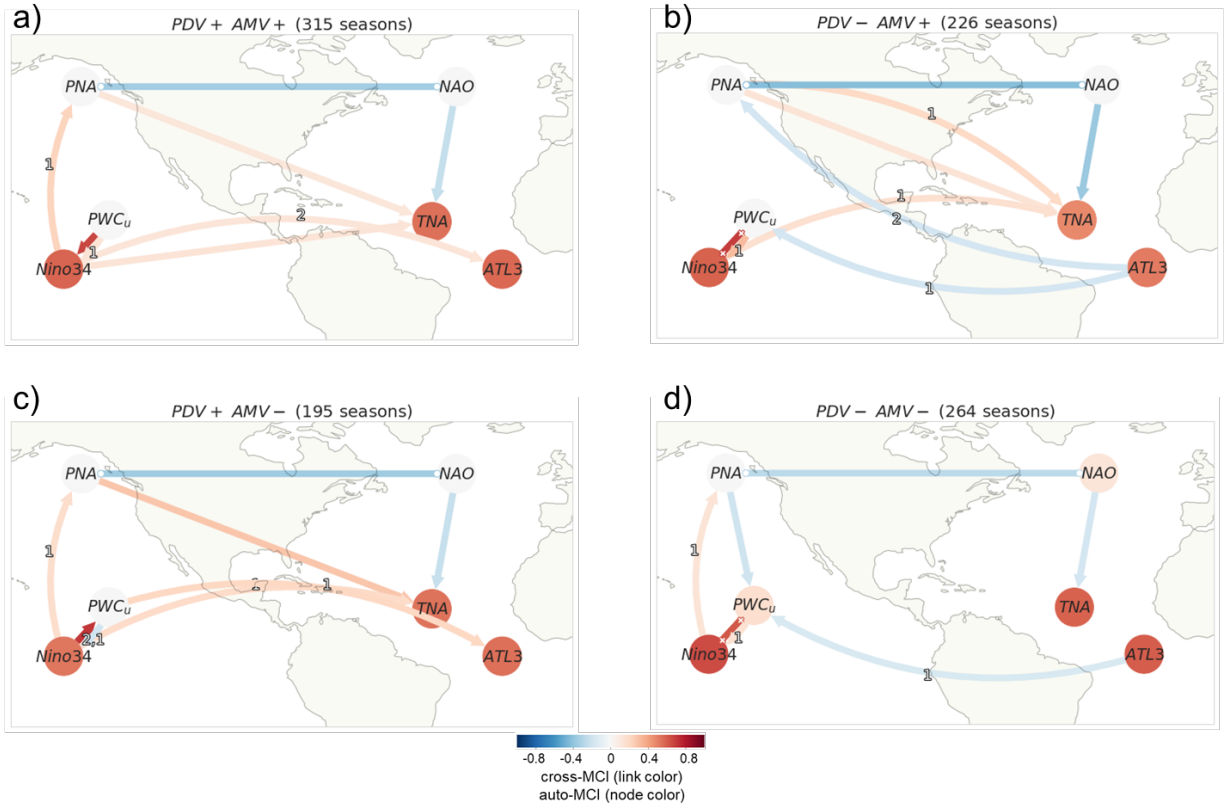

Figure S15. Similar to Fig. S7 but for corresponding to the causal graphs in Fig. 8 (panels a-d here correspond to panels a-d in Fig. 8)